ELSEVIER

PII: S0032-3861(96)00004-9

Polymer Vol. 38 No. 19, pp. 4795–4802, 1997

0032-3861/97/$17.00+0.00

The biaxial drawing behaviour of poly(ethylene terephthalate)

R. G. Matthews, R. A. Duckett and I. M. Ward*
IRC in Polymer Science and Technology, The University of Leeds, Leeds LS2 9JT, UK

and D. P. Jones
ICI Polyester, PO Box 90, Wilton, Middlesborough, Cleveland TS90 8JE, UK
(Revised 29 November 1996)

It is shown that the biaxial drawing of poly(ethylene terephthalate) at temperatures above the glass transition temperature T_g can be satisfactorily described by the Ball model of rubber elasticity (*Polymer*, 1981, **22**, 1010), providing that the chain entanglement density is assumed to be a linear function of the logarithmic shear strain rate. With this assumption the behaviour for uniaxial, constant width and equibiaxial drawing can be fitted by a single set of model parameters. The validity of the network model has been confirmed by photoelastic studies, provided that the draw ratios do not reach a level where strain crystallization occurs to any significant extent. © 1997 Elsevier Science Ltd.

(Keywords: poly(ethylene terephthalate); biaxial drawing; rubber elasticity)

INTRODUCTION

Much previous research has shown that the uniaxial deformation of poly(ethylene terephthalate) (PET) fibres and films can be described in terms of stretching a molecular network[1–5]. In this paper it will be shown that the biaxial stretching of PET can also be described by a molecular network model, that proposed by Ball *et al.*[6].

The present research follows closely that of Sweeney and Ward[7,8] where the biaxial drawing of PVC above T_g was also modelled by the Ball model. It was found that the true stress–strain curves for a wide range of shear strain rates could be reproduced by this model, providing it was assumed that the number of chain entanglements relates linearly to the natural logarithm of the shear strain rate. It was considered particularly satisfactory that the same network parameters then produced good predictions for the three drawing modes.

In the present paper the drawing behaviour of an isotropic amorphous PET is studied at temperatures just above T_g. It was recognized at the outset that there might be complications if crystallization of the PET occurred during the drawing process, and that under these circumstances, the network model could become invalid, or have to be modified. Although the later network model of Edwards and Vilgis[9] incorporates strain hardening due to the finite extensibility of the network, in PET strain induced crystallinity also contributes to strain hardening[10]. In the present research we have, therefore, restricted our quantitative analyses to comparatively low stretch ratios and sought further collaborating evidence for the validity of the molecular network approach by making photoelastic studies of the PET films, using stress-relaxation tests[11,12].

It is an important feature of the curve fitting process that the values for the parameters in the network model are obtained by fitting the true stress–strain curves for constant width drawing where there are two different principal stresses to be fitted to the same model parameters. This has been shown by previous work[7,8] to be a much more effective procedure than either fitting to uniaxial or equibiaxial drawing where one principal stress is measured. Data for uniaxial and equibiaxial drawing has also been obtained to confirm that the parameters found from constant width drawing do predict these cases to a satisfactory degree of accuracy.

THEORY

The Ball tube model of rubber elasticity

According to the rubber elasticity model of Ball *et al.*[6] (henceforth referred to as the Ball model), equation (1), the free energy, F, for a molecular network at a given state of strain is defined by the principal draw ratios λ_1, λ_2 and λ_3:

$$\frac{F}{kT} = \tfrac{1}{2}N_c\sum_i \lambda_i^2 + \tfrac{1}{2}N_s\sum_i\left(\frac{(1+\eta)\lambda_i^2}{1+\eta\lambda_i^2} + \ln(1+\eta\lambda_i^2)\right) \quad (1)$$

The structure of the network is presented by the parameters N_c, the crosslink density N_s, the chain entanglement density and η, a parameter which defines the extent of motion of the entanglements. These entanglements are envisaged as points at which two chains are connected by a slip ring, and η defines the distance along the chains that the slip ring can slide. There are two limiting values for η: zero, where the entanglements act like permanent crosslinks, and infinity, where they make no contribution to the elasticity.

* To whom correspondence should be addressed

The principal stresses, σ_{ii}, corresponding to the state of strain of the rubber, can be calculated from equation (1) using the following relationship:

$$\sigma_{ii} = \lambda_i \frac{\partial F}{\partial \lambda_i} + p \tag{2}$$

where p is a hydrostatic pressure term resulting from the assumed incompressibility. The pressure term is eliminated by noting that the principal stress normal to the film plane, taken to be σ_{22}, is zero in the three drawing modes studied in this investigation, so

$$p = -\lambda_2 \frac{\partial F}{\partial \lambda_2} \tag{3}$$

and therefore

$$\sigma_{33} = \lambda_3 \frac{\partial F}{\partial \lambda_3} - \lambda_2 \frac{\partial F}{\partial \lambda_2} \tag{4}$$

and

$$\sigma_{11} = \lambda_1 \frac{\partial F}{\partial \lambda_1} - \lambda_2 \frac{\partial F}{\partial \lambda_2} \tag{5}$$

Including rate dependence in the Ball model

Because the Ball model is calculated using equilibrium thermodynamics it contains no rate dependent parameters; however, the true stress–strain curves for most thermoplastic polymers are known to be dependent on the rate of deformation[12,13]. The experiments of Brereton and Klein on irradiated polyethylene[13] were performed to investigate the possibility that the Ball model might show some rate dependence, and it was concluded that this is possible if N_c and N_s are rate dependent, but η is not.

Further investigation in this area was undertaken by Sweeney and Ward[7,8] on PVC because, having no chemical crosslinking, the chain entanglement density should be the only rate dependent parameter. It was shown that there was a linear relationship between the number of entanglements and the natural logarithm of the shear strain rate. This suggests that the breakdown of entanglements may occur by a thermally activated process, as observed for PET fibres[14].

Equivalence of drawing modes

For a given deformation mode the level of stress can usually be related to any one of the principal strain rates, but in comparing drawing modes this is no longer adequate. In describing the general deformation of polymers with a rubber network model the concept of equivalent deformations has therefore to be introduced. A more general measure of the total deformation rate is needed that combines the effects of all the applied principal strain rates. Following previous papers by Sweeney and Ward[7,8] it is assumed that the octahedral shear strain rate is the appropriate measure of deformation rate, i.e. by performing different drawing modes at the same octahedral shear strain rates, results from all drawing modes can be described by the same set of model parameters.

The appropriate octahedral shear strain rate is obtained by transferring the strain rate tensor on to the axis set defined by the octahedral stresses. The relationship between the octahedral shear strain rate $\dot{\gamma}$ and the principal strain rates, $\dot{e}_{ii}$ for $i = 1$, 2 and 3, is given as[7,8]

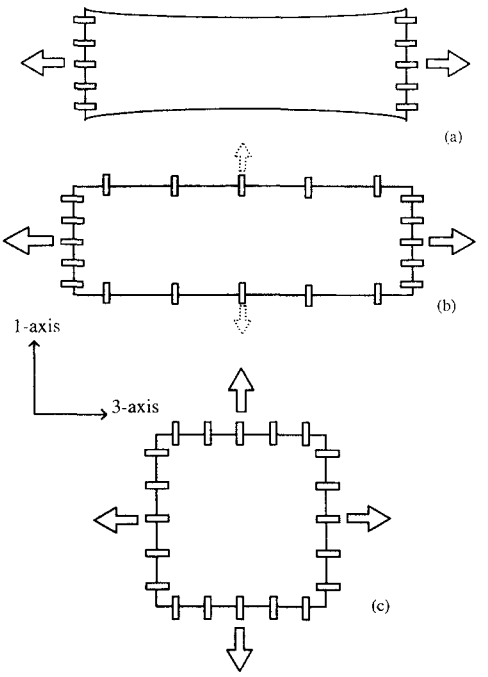

Figure 1 Diagram of the methods used to achieve the three drawing modes: (a) uniaxial; (b) constant width; (c) equibiaxial

$$\dot{\gamma} = \frac{-1}{9\tau_{oct}}((\sigma_{33} - 2\sigma_{11})\dot{e}_{11} + (\sigma_{33} + \sigma_{11})\dot{e}_{22} + (\sigma_{11} - 2\sigma_{33})\dot{e}_{33}) \tag{6}$$

where σ_{11} and σ_{33} are the principal stresses in the 1 and 3 axes, respectively, and $\sigma_{22} = 0$, as shown in *Figure 1*, and the octahedral shear stress τ_{oct} is defined by

$$\tau_{oct} = \tfrac{1}{2}\sqrt{2(\sigma_{11}^2 + \sigma_{33}^2 - \sigma_{11}\sigma_{33})} \tag{7}$$

The rate of deformation was defined as the rate of change in the draw ratio, with principal strain rates $\dot{e}_{ii} = \dot{\lambda}_i$, so for uniaxial drawing in the 3-axis direction the shear strain rate was found to be

$$\dot{\gamma} = \frac{\sqrt{2}\dot{\lambda}^3}{3}(1 + \tfrac{1}{2}\lambda_3^{-3/2}) = \frac{\sqrt{2}}{3}\frac{d}{dt}(\lambda_3 - \lambda_3^{-1/2}) \tag{8}$$

and for equi-biaxial drawing in the 1–3 plane:

$$\dot{\gamma} = \frac{\sqrt{2}\dot{\lambda}_3}{3}(1 + 2\lambda_3^{-3}) = \frac{\sqrt{2}}{3}\frac{d}{dt}(\lambda_3 - \lambda_3^{-2}) \tag{9}$$

The situation when drawing at constant width is more complicated because it involves less symmetry, so the shear strain rate is dependent on the ratio of the principal stresses, $a = \sigma_1/\sigma_3$, as shown in the following equation:

$$\dot{\gamma} = \frac{\sqrt{2}\dot{\lambda}_3}{3\sqrt{a^2 - a + 1}}\left(1 - \frac{a}{2} + \frac{1+a}{2}\lambda_3^{-2}\right) \tag{10}$$

Equations (8)–(10) define how the strain rates have to be varied during drawing to produce a constant octahedral shear strain rate. The equation relating to the constant width drawing contains the ratio of the principal stresses in the film plane. Direct measurements in trial experiments[7] suggested that $a \approx 1/3$ and this mean value of a was used rather than the actual values of stresses in the control loop. It was found that the error in

the shear strain rate introduced by this is only about 2%, so this approach was used here.

Photoelastic behaviour of a rubber-like network

The photoelastic behaviour of the PET film was examined to gain evidence to support the presence of a rubber-like network. The birefringence (Δn) of an extended Gaussian rubber-like network has been shown[11,15] to have a linear dependence on the true stress (σ), so

$$\Delta n = C\sigma \tag{11}$$

where

$$C = \frac{2\pi}{45kT}\frac{(n_0^2+2)^2}{n_0}(\alpha_1 - \alpha_2) \tag{12}$$

C is the stress optical coefficient, n_0 is the average refractive index and $(\alpha_1 - \alpha_2)$ is the polarizability of a random link. Doi and Edwards[16] have also found that the linear relationship between stress and birefringence can, in certain conditions, be obtained for non-Gaussian networks. It should be noted, however, that the stress optical law[16] for non-Gaussian rubbers may not relate to polymers close to the glass transition, as in the experiments described in this paper, because it breaks down at high stresses. It is, therefore, of interest to undertake birefringence measurements to explore the stress–optical behaviour of the deformed samples, including stress relaxation experiments, and compare the results with those of previous studies of the stress optical behaviour of PET.

EXPERIMENTAL

Biaxial drawing of PET film

The 700 μm thick isotropic and amorphous PET film examined in this paper, supplied by ICI, had an initial density of 1337 kg m^{-3}, an initial birefringence of 0.001 and an intrinsic viscosity of 0.6. The drawing experiments were performed using a rig, designed and built in-house[7,8], which could measure the loads acting in the draw directions of samples drawn within a high temperature air oven. The motors driving the grips along the two perpendicular stretching axes can be programmed to move independently at variable rates so that constant shear strain rates can be achieved.

The samples drawn in the biaxial drawing rig are 19 cm square and they are gripped for each drawing mode in the manner shown in *Figure 1*. For uniaxial drawing only two opposite edges need to be gripped and the grips are free to slide perpendicular to their drawing axis so that the sample can contract in the transverse direction.

Curve fitting procedure

To fit the Ball model[6] to the experimental data using a least squares minimization program, initial estimates of the model parameters are needed. These were obtained using Mooney–Rivlin plots where the reduced stress:

$$\sigma^* = \frac{\sigma}{(\lambda_{max}^2 - \lambda_{min}^2)} \tag{13}$$

is plotted against the inverse of the draw ratio which gives a linear plot for rubber-like behaviour. Therefore

$$\sigma^* = C_1 + C_2/\lambda \tag{14}$$

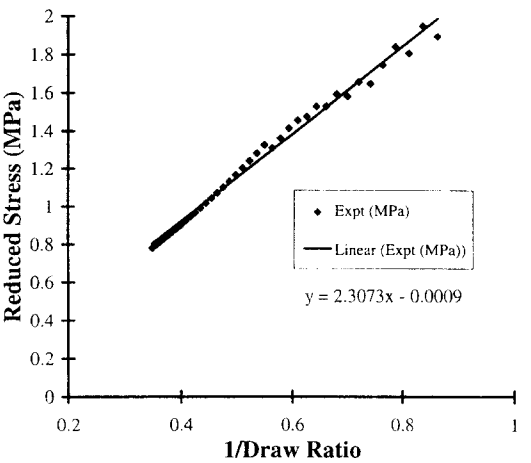

Figure 2 A Mooney–Rivlin plot obtained from the constant width drawing of isotropic PET film drawn at an octahedral shear strain rate of 0.135 s^{-1} at 85°C

where C_1 and C_2 are empirical constants called the Mooney–Rivlin coefficients, which can be related approximately to N_c and N_s, where $N_c = C_1/kT$ and $N_s = C_2/kT$. The estimate of N_s, however, is not strictly correct because C_2 also relates to the link effectiveness.

The Mooney–Rivlin plots obtained from the deformation of PET are not linear over the whole strain range because at high strains there is a sharp upturn where strain hardening occurs. Therefore, only the data points on the initial linear part of the curve were used to give values for N_c and N_s. A specimen Mooney–Rivlin plot obtained from the constant width drawing of PET is included in *Figure 2*.

No estimate for η is obtained from the Mooney–Rivlin plots so to check that the least squares fit is not sensitive to the initial guess of η it was performed twice with different η values. The guesses of η used in the fits were $\eta = 0$, where the slip-links are acting as crosslinks, and $\eta = 0.2342$, a value determined by Ball *et al.*[6], which minimized the free energy in the model. The results showed that the parameter values obtained from the curve fitting were to a very good approximation independent of the initial guess of η.

Strain rate dependence of the model parameters

Samples of PET were drawn at constant width and constant octahedral shear strain rates between 0.5 s^{-1} and 5.0×10^{-4} s^{-1}. Each of the true stress–strain curves was then fitted to the Ball model as described above, and the values for the network parameters were examined for shear strain rate dependence.

The 85°C drawing temperature was chosen on the basis of previous work[17], which has shown that PET shows significant rubber-like behaviour at this temperature. Below 85°C PET is in the glass transition region where there is a considerable viscous contribution to the drawing stress, and too far above 85°C crystallization occurs at modest strains with the effect of modifying the strain hardening behaviour. Constant width drawing experiments were used because more accurate values for the network parameters are obtained from the curve fitting[7,8]. The two different principal stresses must relate to the same model parameters and the need to fit both stresses narrows the ranges of possible values. The maximum shear strain rate investigated was 0.5 s^{-1}

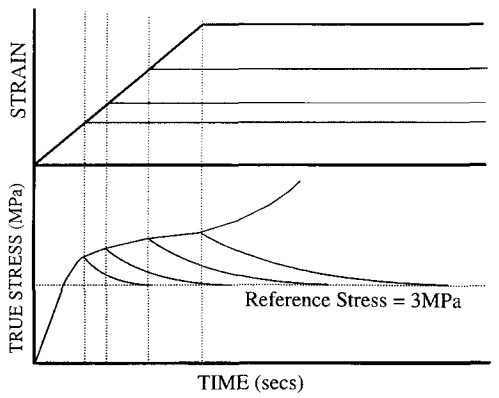

Figure 3 A schematic diagram of the relationship between the true stress and the strain during the stress relaxation tests

because this is the maximum practical rate of drawing on the biaxial drawing rig. The lowest shear strain rate examined was $5.0 \times 10^{-4}\,s^{-1}$ because below this the PET film appears to exhibit viscous flow rather than rubber-like behaviour[10].

Equivalence of different drawing modes

To show that the three drawing modes could be performed equivalently, samples were drawn uniaxially, equibiaxially and at constant width over a range of shear strain rates. The true stress–strain data were then fitted to the Ball model, and the rate dependence of the model parameters was found for all three drawing modes. The drawing was performed at 85°C and at constant shear strain rates between $0.5\,s^{-1}$ and $5.0 \times 10^{-4}\,s^{-1}$ for the reasons given above.

Stress relaxation behaviour

Samples of the isotropic PET film were drawn uniaxially at 85°C to draw ratios between 1.7 and 3.3 to produce a range of orientations and true stresses. The samples were then held at constant length, at 85°C, allowing the stress to relax until they were all at the same true stress and then they were rapidly cooled below T_g to halt the process. If the behaviour is rubber-like they should all have the same level of birefringence. *Figure 3* is a schematic diagram showing the strain–time and the stress–time plots for the stress relaxation tests described above.

The experiment was performed on an Instron tensile testing machine at a strain rate of $0.03\,s^{-1}$, which is comparable to the rates used in the biaxial drawing experiments. To confirm the significance of the results the birefringences of the samples before the relaxation also had to be measured, so some samples were quenched without allowing the stress to relax. The principal refractive indices and therefore the birefringences of all the tested samples were measured using an Abbe refractometer.

RESULTS AND DISCUSSION

Strain rate dependence

From the curve fitting of the experimental data clear patterns were observed in the model parameters. The value of N_c was found to be zero, which is consistent with the absence of chemical crosslinking in PET and removes the crosslink term in equation (1). Examples of the fits of

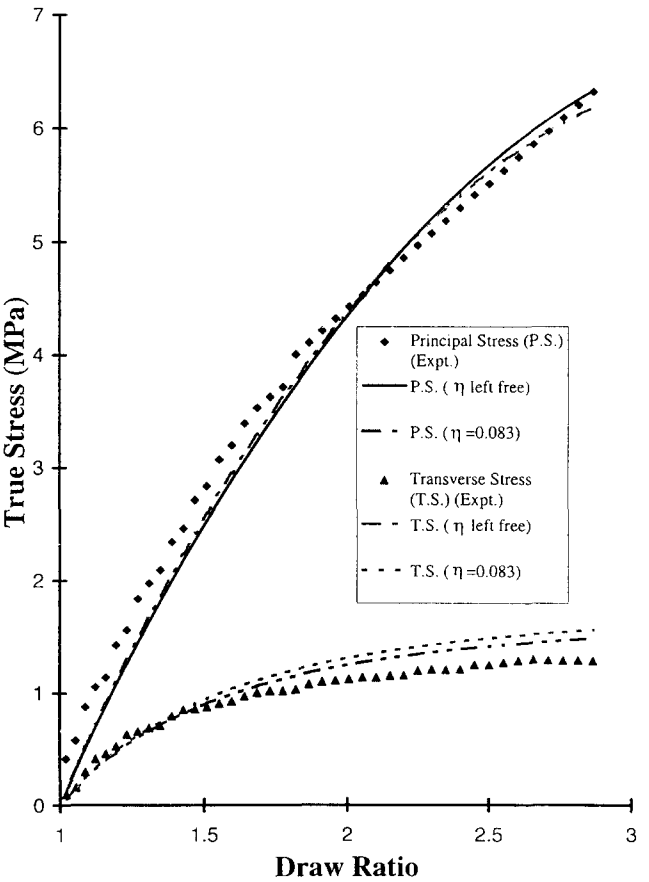

Figure 4 Fitting the Ball model to the constant width drawing of PET at 85°C at a constant shear strain rate of $0.135\,s^{-1}$ where $N_c = 0$ and η and N_s are left free, and $\eta = 0.0833$ and N_s is left free [principal stress (P.S.) is stress in 3-axis; transverse stress (T.S.) is stress in 1-axis]

the constant width true stress–strain curves to the model are given in *Figures 4–6* where $N_c = 0$ and N_s and η were allowed to vary.

In *Figure 7* the values obtained from the fits for N_s are plotted against the natural logarithm of the shear strain rate (full line) showing that there is a clear linear relationship. The rate dependence of η, *Figure 8*, shows a slight increase with increasing shear strain rates. The effect is very small, however, and is considered negligible in comparison with the experimental errors, so η can be treated as a constant at 0.083. In *Figures 4–6* the fits of the experimental data to the model, holding η constant at 0.083, are also shown, and it is seen that this constraint has little effect on the quality of the fits. The values obtained for the chain entanglement density, N_s, are also shown to be only minimally affected by the assumption of constant η (see *Figure 7*).

The curve fitting shows that N_s is the only rate dependent parameter and that it is linearly related to the octahedral shear strain rate, so that we can write

$$N_s kT = 0.398 \ln(\dot{\gamma}/\dot{\gamma}_0) + 3.252 \qquad (15)$$

for shear strain rates in the range $5 \times 10^{-3} - 0.5\,s^{-1}$, where $\dot{\gamma}_0$ is chosen as an octahedral shear strain rate of $1\,s^{-1}$. These results obtained for PET are similar to those obtained for PVC by Sweeney and Ward[7,8].

There are two consistent discrepancies between the model curves and the experimental data, *Figures 4–6*, the first being that the principal stress is underestimated over the first section of the curves. The second discrepancy is

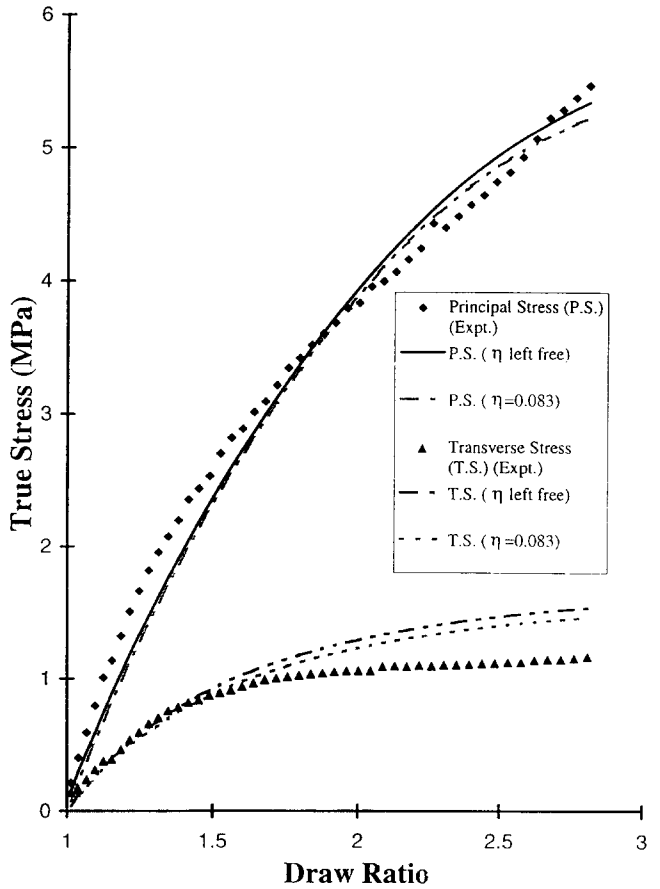

Figure 5 Fitting the Ball model to the constant width drawing of PET at 85°C at a constant shear strain rate of $0.018\,s^{-1}$ where $N_c = 0$ and η and N_s are left free, and $\eta = 0.0833$ and N_s is left free (P.S. is stress in 3-axis; T.S. is stress in 1-axis)

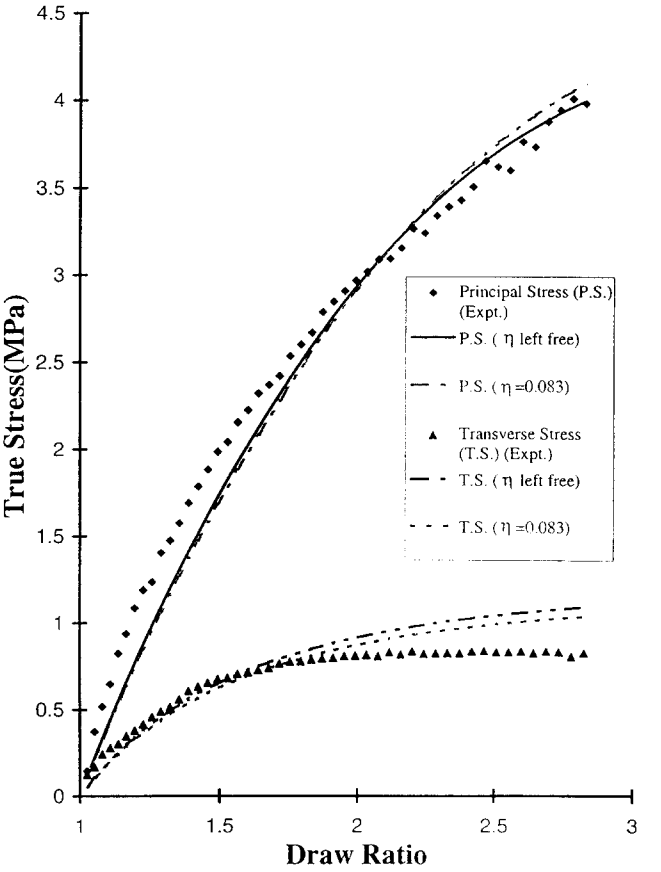

Figure 6 Fitting the Ball model to the constant width drawing of PET at 85°C at a constant shear strain rate of $0.0067\,s^{-1}$ where $N_c = 0$ and η and N_s are left free, and $\eta = 0.0833$ and N_s is left free (P.S. is stress in 3-axis; T.S. is stress in 1-axis)

the overestimate of the principal stress in the transverse direction by the model. This occurs because the data were not normalized before the least squares fits as it was decided to fit preferentially to the larger principal stress, which has a lower percentage error.

Equivalence of drawing modes using the same constant shear strain rate

The rate dependences of the model parameters obtained from curve fitting to uniaxial and equibiaxial draws at 85°C were compared to those from the constant width drawing experiments described above. The fitting to uniaxial and equibiaxial data is less accurate than for the constant width drawing so assumptions were made to simplify the situation. It was proposed that the values of the rate independent parameters N_c and η obtained from the constant width experiments should be used in the curve fitting to the data from the other drawing modes.

Examples of the excellent fits obtained to the experimental data when only N_s is allowed to vary with the shear strain rate are shown in *Figures 9* and *10*. In *Figure 11* comparison is made of the rate dependence of N_s for all three drawing modes and it shows that they exhibit the same dependence. This result confirms the suggestion that different drawing modes can be performed equivalently by drawing at the same shear strain rates.

Characteristics of the network in the PET film

The entanglement density obtained from the curve fitting procedure can be used to calculate the number of

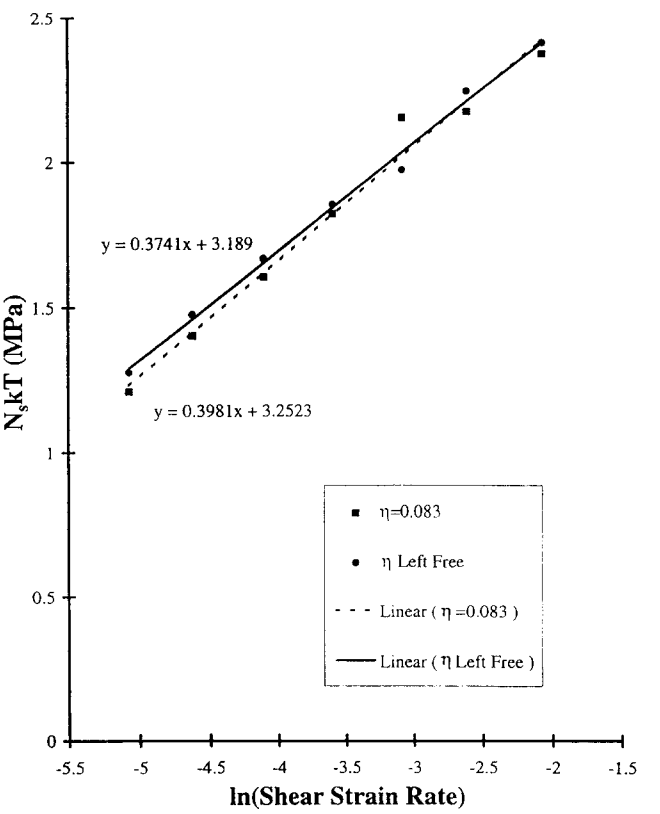

Figure 7 The variation of $N_s kT$ with the shear strain rate for the constant width drawing of PET at 85°C assuming $N_c = 0$ and η is free, and $\eta = 0.083$

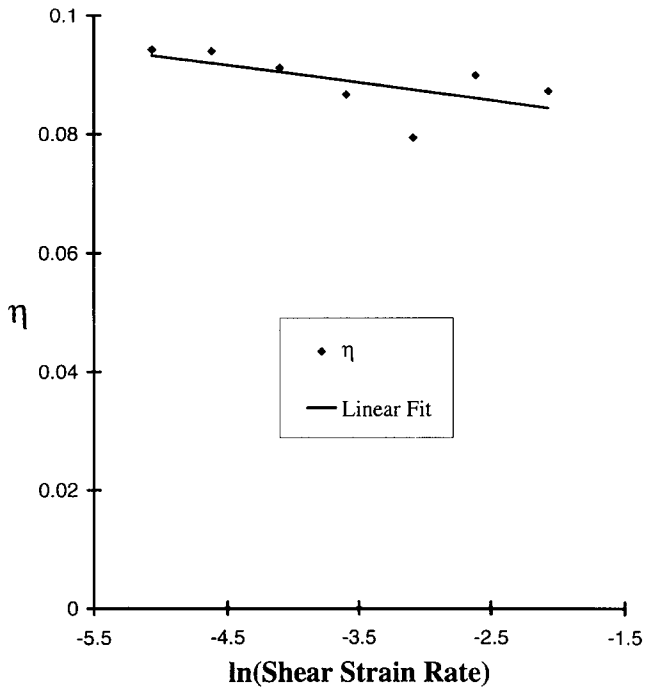

Figure 8 The variation of η with the shear strain rate for the constant width drawing of PET at 85°C assuming $N_c = 0$

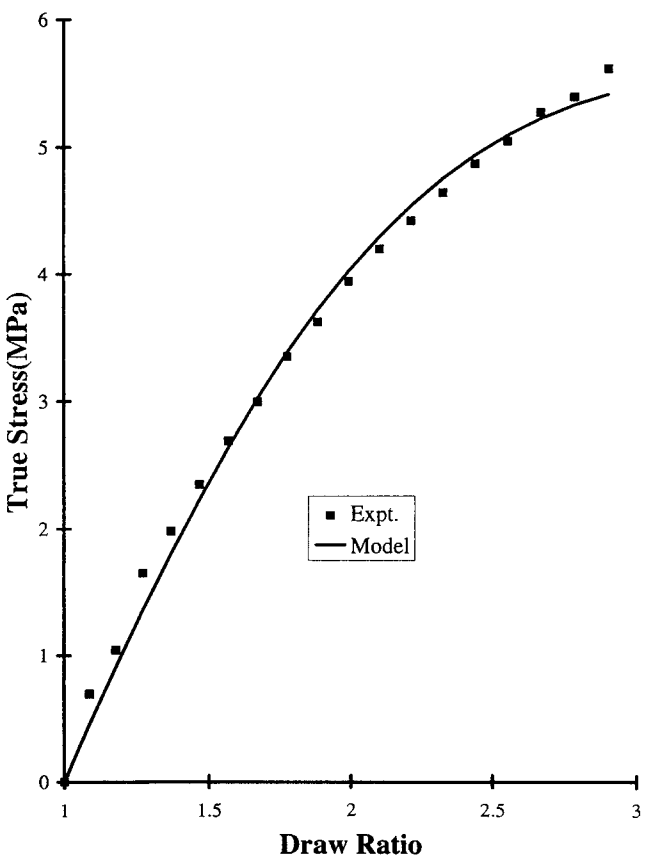

Figure 9 The best fit obtained to the uniaxial drawing of PET at a constant shear strain rate of $2.5 \times 10^{-2}\,s^{-1}$ using parameters from the constant width results where $N_c = 0$, $\eta = 0.083$ and N_s is left free

monomers per chain, n, which previous research has suggested should be around 15[4,17]. The approach taken in this paper results in n being a rate dependent parameter with values, shown in *Figure 12*, that are

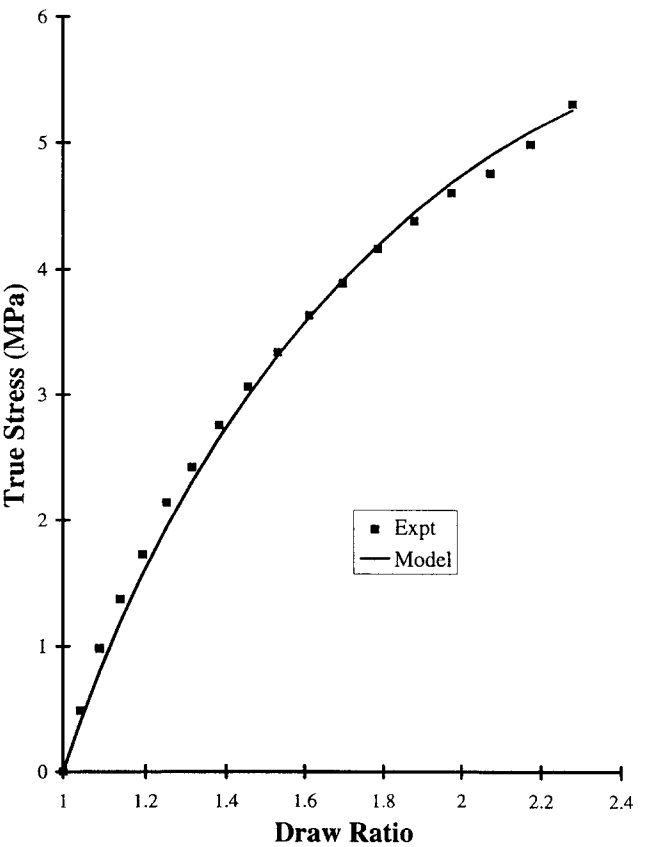

Figure 10 The best fit obtained to the equibiaxial drawing of PET at a constant shear strain rate of $2.5 \times 10^{-2}\,s^{-1}$ using parameters from the constant width results where $N_c = 0$, $\eta = 0.083$ and N_s is left free

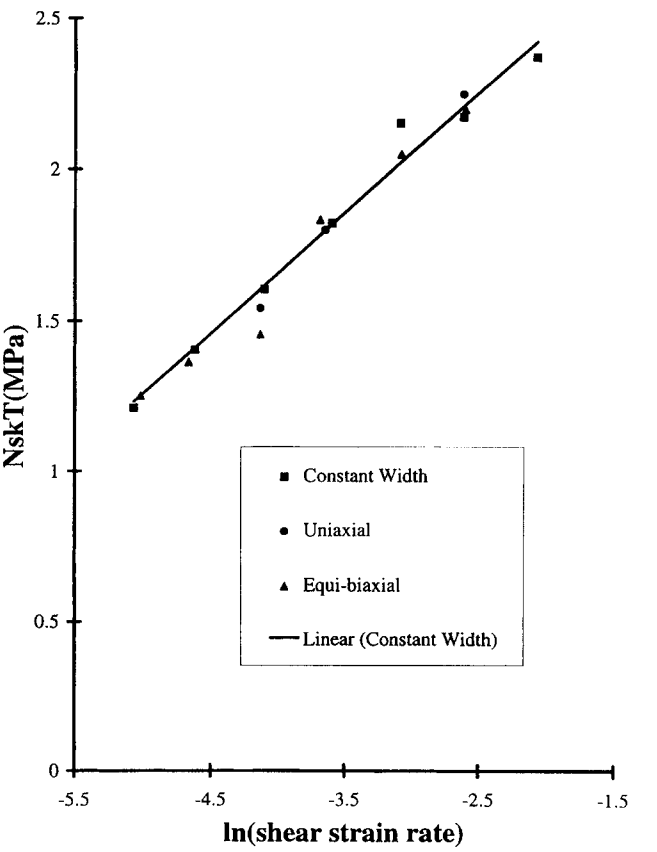

Figure 11 Comparing the $N_s kT$ values obtained from curve fitting to the true stress–strain curves for PET drawn at 85°C assuming $N_c = 0$ and $\eta = 0.083$

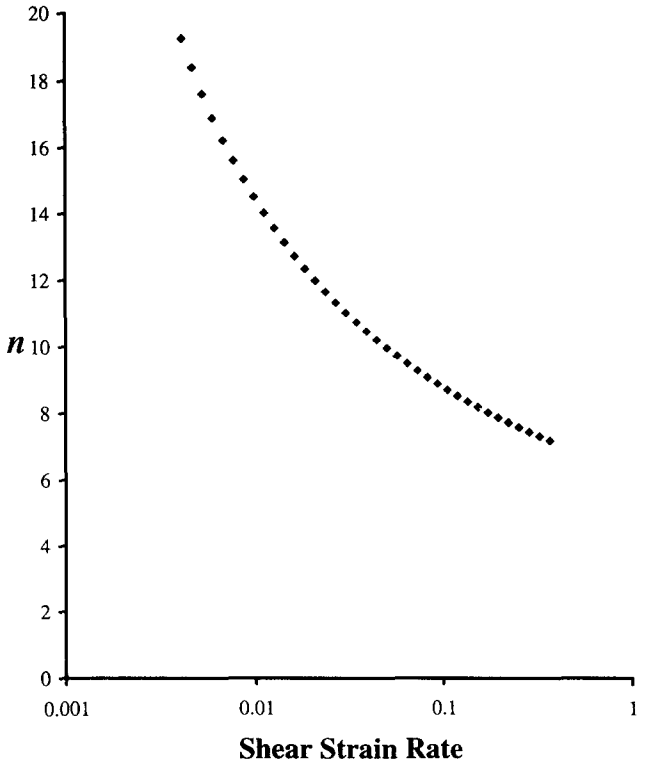

Figure 12 The variation in the number of monomers, n, between crosslinks with the shear strain rate for the drawing of PET at 85°C

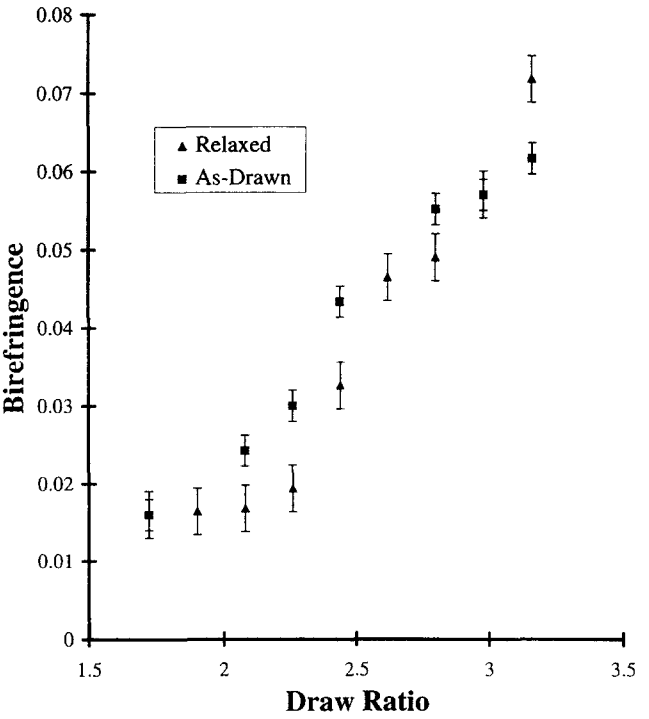

Figure 13 The effect on the birefringence of allowing PET samples drawn uniaxially at 85°C at a shear strain rate of $0.04\,s^{-1}$ to relax at 85°C to the same true stress

independent of the drawing mode. This shows that n increases from 7 to 17 as the shear strain rate is reduced from 0.135 to $0.0067\,s^{-1}$, so there is no major discrepancy between the two approaches.

Stress relaxation behaviour

In *Figure 13* the birefringence of the drawn PET samples, before and after relaxation, is plotted against the applied draw ratio. It shows that at draw ratios below 2.2 the birefringence of the samples relaxed to a fixed stress is independent of the final draw ratios; this is a feature of rubber-like behaviour.

At draw ratios higher than 2.2 the birefringence of the relaxed samples increases with increasing draw ratio, probably due to strain crystallization locking-in the network extension. At draw ratios above 3 the sample birefringence actually increases during the stress relaxation test because annealing probably increases the crystallinity and the orientation for these samples. These results suggest that at draw ratios above 2.2 the rubber-like behaviour of the PET is perturbed by strain induced crystallization rather than the stress optical law breaking down due to the high stress level[16].

If the stress–optical coefficient:

$$C = \frac{\Delta n}{\sigma} \tag{16}$$

is calculated from the initial plateau region of the birefringence against the draw ratio curve for the relaxed samples, shown in *Figure 13*, it can then be compared to the value predicted from the results of previous workers.

The literature[4] gives values for PET of 1.58 for the average refractive index (n_0), and $1.67 \times 10^{-29}\,m^3$ for the polarizability of a random link ($\alpha_1 - \alpha_2$), which results in a stress optical coefficient of $6.0 \times 10^{-9}\,Pa^{-1}$ at 85°C. The stress relaxation tests give a value for the birefringence in the plateau region of 0.016 for the samples relaxed to a true stress of 3.0 MPa. This gives a value for the stress–optical coefficient of $5.5 \times 10^{-9}\,Pa^{-1}$, which agrees well with the predicted value. Temperature variations in the experiment and the fact that the predicted value does not take into account any strain rate dependence could easily account for any small differences.

One of the basic assumptions of the work described in this paper is that the stress developed in the samples is due entirely to the extension of a network. The fall in the stress as the samples relax must, therefore, be entirely due to a relaxation of the network. There are two possible explanations of the fall in the stress, in terms of the classical network theory, because the stress and the birefringence are both functions of $N(\lambda^2 - \lambda^{-1})$. Therefore, it is either due to a decrease in the extension of the network or in the cross-link density, but this experiment cannot distinguish between the two.

Extending the model to different regimes

The experiments described in this paper were performed at 85°C because previous work shows that the behaviour of PET film at this temperature is rubber-like without any viscous contribution[17]. This was shown most strongly by the observation that the final drawing stress and the shrinkage stress obtained from samples drawn at 85°C are the same. Therefore, working at this temperature allows the rate dependence of the network parameters to be studied under conditions where there is no rate dependent viscous contribution.

It is acknowledged that the present model cannot be used for measurements undertaken in conditions where there is a viscous contribution to the drawing stress. The situation in PET at 85°C is similar to that for PVC at

90°C, previously studied by Sweeney and Ward[7], where it was shown that an alternative model, of an Eyring viscous flow process in parallel with a simple rubber-like network (rate independent entanglement density), could not describe the stress–strain behaviour. A characteristic of this alternative model is that after an initial transient period the viscous contribution to the stress should become constant, and the change of stress with draw ratio should be due to the rate in independent network contribution. Therefore, if two draws are performed at different rates the model predicts that after the transient period the true stress–strain curves should be parallel. Sweeney and Ward found that this was not the case and that the true stress–strain curves could only be modelled if the network contribution was also rate dependent.

Sweeney and Ward also found that there was a qualitative difference in behaviour for PVC drawn at the two temperatures of 84 and 90°C. At 84°C, which is within the glass transition range, there is a yielding type behaviour with an initially high slope in the stress–strain curve followed by a rapid change to a lower slope. To model the 84°C results, Sweeney and Ward introduced a viscous component in parallel with the time dependent network and in series with an elastic response. The 84°C data for PVC are similar in kind to results recently reported for PET by Buckley and co-workers[18,19]. Buckley *et al.*[18] have modelled their data, which show a yield point, by assuming that the total stress consists of a rubber-like contribution with fixed entanglement density, together with a glass-like contribution incorporating flow. The rate dependence arises both from the glass component and from entanglement-slippage, an extra viscous deformation at low strains. It would seem that the 'parallel', viscous component is negligibly small in the temperature/strain rate window explored in the current study.

CONCLUSIONS

It has been shown that the Ball model can be modified to describe the rate dependence of the drawing behaviour of PET simply by making the entanglement density a linear function of the natural logarithm of the shear strain rate. The model cannot, however, be used to describe the stress–strain curves much above a draw ratio of 2.2, where strain hardening is observed. It is important to determine the model parameters by fitting both the axial and transverse stresses in experiments based on drawing at constant width. Once determined these parameters can then be used to calculate the behaviour in uniaxial and biaxial drawing with good precision at the same equivalent shear rate. The rate dependent density of entanglements has been used to calculate the number of monomers per chain and this is in general agreement with the published data even though it is also rate dependent.

Evidence supporting the presence of a molecular network in the PET film was obtained from the stress relaxation tests. These tests also showed the limitations of the network approach because, at high draw ratios, strain induced crystallization disrupts the rubber-like behaviour. This clearly indicates that a purely network model cannot be used to describe the true stress–strain curves at high draw ratios.

ACKNOWLEDGEMENTS

R.G.M. would like to thank SERC and ICI Films for supporting his CASE Ph.D. studentship. The authors also thank ICI Films for supplying materials for the project and Dr J. Sweeney of the IRC and Dr D. J. Blundell of ICI plc for many helpful discussions during the course of the work.

REFERENCES

1. Ward, I. M., *Polym. Eng. Sci.*, 1984, **24**, 724.
2. Buckley, C. P., Jones, D. C. and Jones, D. P., *Polymer Processing Society, 9th Meeting*, Manchester, UK, The Polymer Processing Society, 1993.
3. Boyce, M. C., Parks, D. M. and Argon, A. S., *Int. J. Plast.*, 1989, **5**, 593.
4. Long, S. D. and Ward, I. M., *J. Appl. Polym. Sci.*, 1991, **42**, 1921.
5. Brody, H., *J. Macro. Sci. Phys.*, 1983, **B22**, 19.
6. Ball, R. C., Doi, M., Edwards, S. F. and Warner, M., *Polymer*, 1981, **22**, 1010.
7. Sweeney, J. and Ward, I. M., *Polymer*, 1995, **36**, 299.
8. Sweeney, J. and Ward, I. M., *Trans. Inst. Chem. Eng.*, 1989, **5**, 593.
9. Edwards, S. F. and Vilgis, T. A., *Polymer*, 1986, **27**, 483.
10. Matthews, R. G., Ph.D. thesis, University of Leeds, UK, 1995.
11. Treloar, L.R.G., *The Physics of Rubber Elasticity*, 3rd edn. Clarendon Press, Oxford, UK, 1975, pp. 174–209.
12. Ward, I. M., *Mechanical Properties of Solid Polymers*, 2nd edn. John Wiley, Chichester, UK, 1983, pp. 62–107.
13. Brereton, M. G. and Klein, P. G., *Polymer*, 1988, **29**, 970.
14. Pinnock, P. R. and Ward, I. M., *Trans. Faraday Soc.*, 1966, **62**, 1308.
15. Kuhn, W. and Grün, F., *Kolloidzschr.*, 1942, **101**, 248.
16. Doi, M. and Edwards, S. F., *The Theory of Polymer Dynamics*. Clarendon Press, Oxford, UK, 1986, p. 221.
17. Gordon, D. H., Duckett, R. A. and Ward, I. M., *Polymer*, 1994, **35**, 2554.
18. Buckley, C. P., Jones, D. C. and Jones, D. P., *Polymer*, 1996, **37**, 2403.
19. Adams, A. M., Buckley, C. P. and Jones, D. P., *Proceedings of the Polymer Processing Society, European Regional Meeting*, Strasbourg, The Polymer Processing Society, 1994.